
PERGAMON

Journal of Quantitative Spectroscopy & Radiative Transfer 68 (2001) 57–73

Journal of Quantitative Spectroscopy & Radiative Transfer

www.elsevier.com/locate/jqsrt

A superposition technique for deriving mean photon scattering statistics in plane-parallel cloudy atmospheres

S. Platnick[a,b,*]

[a]*Joint Center for Earth Systems Technology, University of Maryland Baltimore County, Baltimore, MD, USA*
[b]*Code 913, NASA Goddard Space Flight Center, Greenbelt, MD 20771, USA*

Received 2 June 1999

Abstract

Photon transport in a multiple scattering medium is critically dependent on scattering statistics, in particular the average number of scatterings. A superposition technique is derived to accurately determine the average number of scatterings encountered by reflected and transmitted photons within arbitrary layers in plane-parallel, vertically inhomogeneous clouds. As expected, the resulting scattering number profiles are highly dependent on cloud particle absorption and solar/viewing geometry. The technique uses efficient adding and doubling radiative transfer procedures, avoiding traditional time-intensive Monte Carlo methods. Derived superposition formulae are applied to a variety of geometries and cloud models, and selected results are compared with Monte Carlo calculations. Cloud remote sensing techniques that use solar reflectance or transmittance measurements generally assume a homogeneous plane-parallel cloud structure. The scales over which this assumption is relevant, in both the vertical and horizontal, can be obtained from the superposition calculations. Though the emphasis is on photon transport in clouds, the derived technique is applicable to any multiple scattering plane-parallel radiative transfer problem, including arbitrary combinations of cloud, aerosol, and gas layers in the atmosphere.

Keywords: Cloud remote sensing; Multiple scattering; Scattering statistics; Adding/doubling method of technique; Photon diffusion

1. Introduction

Determination of photon path length distributions, including mean path length, average number of scatterings, etc., has been pursued by a number of investigators over the years with application to

* Correspondence address. Code 913, NASA GSFC, Greenbelt, MD 20771, USA.
E-mail address: platnick@climate.gsfc.nasa.gov (S. Platnick).

0022-4073/00/$ - see front matter
PII: S0022-4073(00)00015-7

molecular and cloudy atmospheres. Interests include atmospheric line absorption [1], comparison with atmospheric absorption calculations obtained from traditional numerical codes [2], and cloud lidar studies where the path length distribution undergone by returning photons is related to the spread in the time delay of the return signal [3].

Monte Carlo techniques can be used to determine the mean optical path of reflected and transmitted radiation from clouds, as well as the path length distribution [4,5]. However, calculations generally require significant computational time for acquiring sufficient photon statistics. Another possible technique is through the inverse Laplace transform of the path absorption integral [1]. This technique can provide the photon path distribution, though numerical difficulties and problems with uniqueness can occur [1,2,6]. Mean path length and other moments can also be found by differentiating the integral equation with respect to single scattering albedo and optical thickness [1,6,7]. The average number of scatterings is, of course, closely related to the average photon path length (first moment of path length distribution) and is a useful quantity in its own right.

A fast and efficient means of calculating the average number of scatterings in arbitrary layers of plane-parallel, vertically inhomogeneous, cloudy atmospheres has been developed. The new technique is derived from superposition principles and can be implemented in a straightforward way with standard adding/doubling numerical routines. The superposition formulae are applicable to conservative or absorbing layers with arbitrary phase functions. The vertical distribution of layer scatterings, as well as the average number of scatterings for the overall cloud, can be determined for arbitrary incident illumination and for emerging photons reflected or transmitted into specific directions (e.g., bidirectional reflectance and transmittance) or into a hemisphere (flux reflectance and transmittance). Calculations using the superposition formulae have been made in visible and near-infrared cloud remote sensing bands, for clouds of varying optical thickness and liquid water droplet size profiles. In this paper we show selected results and comparisons with Monte Carlo calculations. Though the emphasis is on terrestrial clouds, the technique is suitable for any general plane-parallel atmosphere with absorbing and scattering layers.

Several applications to cloud remote sensing were the impetus for this work. First, the vertical distribution of photon scattering numbers can be used to determine the effect of vertically inhomogeneous cloud droplet sizes on retrievals. Second, the average number of scatterings is useful for estimating horizontal transport in plane-parallel layers. Both results can aid in understanding the effect of heterogeneous clouds fields on remote sensing problems by giving the relevant scales over which homogeneous, plane-parallel assumptions need be valid. These applications are the subject of ongoing studies.

The superposition formulae are derived in Section 3. These derivations are couched in the adding/doubling vector–matrix notation developed by Twomey et al. [7,8] and Twomey [9]. Though the notation is straightforward, the derivations are quite general and all equations should be easily renderable to other adding/doubling formulations (e.g., Hansen and Travis [10]). A short summary of the notation is described in Section 2, though the above references should be consulted for a complete discussion. However, while important for the calculations presented in Section 4, proficiency with this notation is not essential to understanding the concepts of Section 3 (a simple two-stream version of the derivation is satisfactory for such purposes). An application to cloud remote sensing is described in Section 5.

2. Vector–matrix notation

In the Twomey adding/doubling method [7–9], radiation at any level in a plane-parallel medium is separated into upward and downward propagating intensity (radiance) beams represented by vectors, e.g., **u** and **d**, respectively. Elements of these vectors indicate the average intensity within some chosen μ-bin, where μ is the cosine of the zenith angle (unlike other doubling techniques where matrix formulations are derived with vector elements being the intensity at discrete μ values). For instance, in the current work, ten equal-width bins were chosen for each hemisphere with central values of $\mu_i = 0.05, 0.15, \ldots, 0.95$ for $i = 1, 2, \ldots, N$ with $N = 10$. This constitutes a 20-stream computation. The redirection of radiation from a particular μ-bin into all other μ-bins is given by the columns of a reflectance matrix, **S**, and two transmittance matrices, one for diffuse and one for directly transmitted radiation, **T** and **E**, respectively. Each matrix accounts for scattering into a hemisphere and is therefore of size 10×10 in this study. As an example, consider some isolated plane-parallel medium with a known reflectance matrix **S** which is illuminated by an incident downward propagating intensity vector **d**. Then the product $\mathbf{u} = \mathbf{Sd}$ gives the upward propagating reflected intensity vector while $(\mathbf{T} + \mathbf{E})\mathbf{d}$ is a vector describing the total transmitted intensity field. In other words, the elements i,j of the matrices gives the scattered intensity into the μ_i direction due to intensity incident from the μ_j direction. The adopted sign of μ is not important with the separation of radiation into two hemispheres, as long as its understood that **S** describes incident radiation scattered into the same hemisphere, while **T** and **E** describe radiation transmitted into the opposite hemisphere. With azimuthal symmetry, the flux passing through any bin is $2\pi\mu_i I_i \Delta\mu$, where I_i is the intensity in bin μ_i. To account for an incident solar flux (irradiance) with this notation, the average intensity corresponding to an angular bin size centered at $\mu_j = \mu_0$ is set to a value such that its angular-integrated flux is $\mu_j F_0$, where F_0 is the solar flux, while all other elements of the incident vector are zero.

The scattering phase function is transformed directly into this separate hemisphere, plane-parallel geometry matrix notation at the outset, before the adding/doubling procedure begins. Two phase function matrices, termed **B** and **P**, are used for this purpose, where **B** describes single scattering back into the incident hemisphere and **P** for scattering into the opposite hemisphere (cf. [8]). With this method, the angular integration for all incident and scattered plane-parallel geometry directions is done one time only in the calculation of these phase function matrices. For a single-scattering differential layer with the phase function normalized to unity, $\mathbf{S}_{d\tau} = \bar{\omega}_0 \mathbf{M}^{-1} \mathbf{B}\, d\tau$ and $\mathbf{T}_{d\tau} = \bar{\omega}_0 \mathbf{M}^{-1} \mathbf{P}\, d\tau$, where **M** is a diagonal matrix with elements μ_i, $d\tau$ the layer's optical thickness, and $\bar{\omega}_0$ the single scattering albedo. The **B**, **P** matrices have been introduced here for completeness, but methods for their calculation from the phase function are not essential to the derivations that follow; the starting point assumption is that $\mathbf{S}_{d\tau}$ and $\mathbf{T}_{d\tau}$ are known. The **S** and **T** matrices for a finite layer are found by adding/doubling up from the differential layer, while **E** is simply a diagonal matrix with elements $\exp\{-\tau/\mu_j\}$. A non-zero surface reflectance can be represented by an additional reflectance matrix added beneath the cloud, though we concentrate primarily on black surfaces in this study (approximately valid for ocean surfaces in the spectral bands of interest). All matrices and vectors can be decomposed into Fourier components to provide azimuthal detail. However, only the azimuthally independent terms are considered in the present work, which should be sufficient for the pertinent cases of clouds with large orders of scatterings and for verification of the formulae derived in the next section.

A common normalization for scattered intensity is via bidirectional reflectance and transmittance. For an incident solar irradiance in direction μ_j, bidirectional reflectance for an azimuthally independent reflected intensity is given in the present notation as $(N/2)S_{i,j}/\mu_j$, where N is the number of μ-bins, and similarly as $(N/2)(T_{i,j} + E_{i,j})/\mu_j$ for transmittance. Albedo and flux transmittance, found by integrating over the viewing hemisphere, becomes $\sum_{i=1}^{N} \mu_i S_{i,j}/\mu_j$ and $\sum_{i=1}^{N} \mu_i (T_{i,j} + E_{i,j})/\mu_j$, respectively, where μ_i is the viewing direction.

In the case of a two-stream calculation, all vectors and matrices reduce to scalars; **S** becomes the flux reflectance (albedo) and $\mathbf{T} + \mathbf{E}$ the flux transmittance. It may be useful to consider this simplified situation when examining the derivation that follows.

3. The average number of scatterings in arbitrary layers

We wish to derive the average number of scatterings encountered by reflected and transmitted photons within any arbitrary layer of a plane-parallel, vertically inhomogeneous medium via adding/doubling numerical procedures. To the extent that the fundamental derivation follows the incorporation of a differential layer into the interior of a finite cloud, we use the generic term *superposition* to describe the method (*invariant imbedding* is a closely related process, see review by Hansen and Travis [10]). We begin by determining the fraction of incident solar radiation that undergoes a scattering in an infinitesimal layer imbedded between two finite layers. A general schematic for the problem at hand is shown in Fig. 1. Two separate plane-parallel, inhomogeneous layers are shown, each with different reflectance and transmittance matrices. Because we allow for vertical inhomogeneities within each layer, the scattering matrices will in general depend on whether radiation is incident from above or below the layer, indicated by superscripts *a* and *b*, respectively. The surface below layer 2 is assumed to be black for the moment; modification of the equations for a reflecting surface is described at the end of this section.

In the following, the vertical optical path variable is referred to as *optical depth*, τ, measured from cloud top downward, while the term *optical thickness*, τ_c, is used to indicate the overall optical depth to cloud base. For example, we may refer to a cloud level at an optical depth of 5, in a cloud with optical thickness 10. For the sake of clarity, the reader may wish to consider a simple two-stream rendition of the derivation in which case all vectors and matrices can be substituted with familiar scalar equivalents. The derivation proceeds in the following four steps:

3.1. *Determination of intensity vectors* **u** *and* **d**, *at an optical depth of* $\tau = \tau_1$, *for a cloud with total optical thickness* $\tau_c = \tau_1 + \tau_2$

First, consider the upward and downward intensities at the level $\tau = \tau_1$, designated as $\mathbf{u}'$ and $\mathbf{d}'$, respectively, in the absence of the infinitesimal layer. Then $(\mathbf{T}_1^a + \mathbf{E})$ gives the component of $\mathbf{d}'$ due to the initial transmission of incident radiation through layer 1, before interaction with layer 2; likewise $\mathbf{S}_1^b \mathbf{S}_2^a (\mathbf{T}_1^a + \mathbf{E})$ is the next higher-order component of $\mathbf{d}'$ after reflection from the lower and then upper cloud layer (note that the order of the multiplication is important because of the matrix formulation). Accounting for all higher-order reflections between the layers yields the following

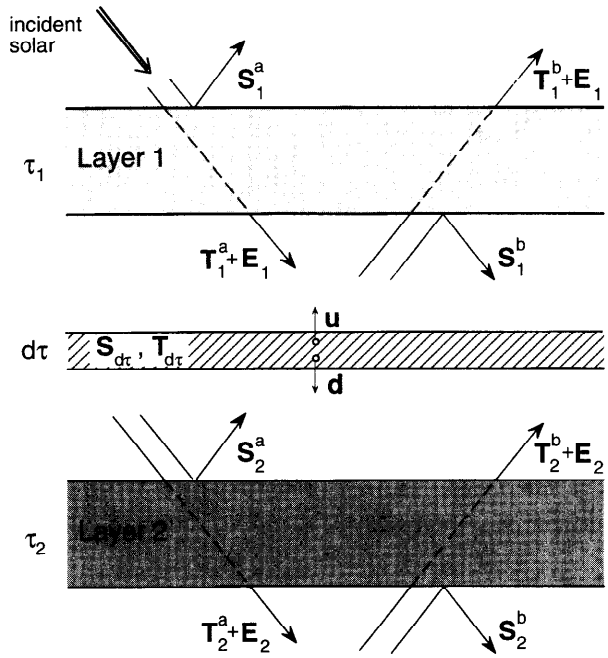

Fig. 1. A homogenous infinitesimal layer of optical thickness $d\tau$, is imbedded between two inhomogeneous plane-parallel layers having total optical thicknesses τ_1 and τ_2. The matrix **S** represents a layer's reflectance, **T** the diffuse transmittance, and **E** the direct transmittance. Because of vertical inhomogeneity, the reflectance and diffuse transmittance for radiation incident from *above* a finite layer is different than for radiation incident from *below* (indicated by subscripts *a* and *b*, respectively). Upward and downward propagating intensities originating in the infinitesimal layer, indicated by the vectors **u** and **d**, respectively, represent only those photons which have had a scattering in the $d\tau$ layer, and are a function of the scattering properties of all three layers.

intensities at the boundary:

$$\mathbf{u}'(\tau_1,\tau_c) = \mathbf{S}_2^a(\mathbf{I} + (\mathbf{S}_1^b\mathbf{S}_2^a) + (\mathbf{S}_1^b\mathbf{S}_2^a)^2 + \cdots)(\mathbf{T}_1^a + \mathbf{E}_1)\mathbf{v}_{\text{inc}},$$

$$\mathbf{d}'(\tau_1,\tau_c) = (\mathbf{I} + (\mathbf{S}_1^b\mathbf{S}_2^a) + (\mathbf{S}_1^b\mathbf{S}_2^a)^2 + \cdots)(\mathbf{T}_1^a + \mathbf{E}_1)\mathbf{v}_{\text{inc}}, \tag{1}$$

where **I** is the identity matrix, and $\mathbf{v}_{\text{inc}}$ represents the downward solar intensity vector at cloud top where all elements of the vector are zero except in the bin corresponding to the solar position $\mu_j = \mu_0$ (in the two-stream case, all quantities are reduced to scalars so $\mathbf{v}_{\text{inc}}$ can be equated with $\mu_0\mathbf{F}_0$ and $\mathbf{I} = 1$). The infinite series, common to all superposition formulations, converges for either non-conservative scattering or finite optical thicknesses.

We now add a homogeneous layer with thickness $d\tau$ between the two finite layers. By making the thickness arbitrarily small, higher-order scatterings with the layers can be ignored and we can consider only those photons which undergo a single scattering in the infinitesimal layer sometime during their multiple passings across the layer 1–2 interface. All such photons contribute a total

intensity at the interface given by

$$\mathbf{u}(\tau_1,\tau_c) = \mathbf{S}_{d\tau}\,\mathbf{d}'(\tau_1,\tau_c) + \mathbf{T}_{d\tau}\,\mathbf{u}'(\tau_1,\tau_c),$$

$$\mathbf{d}(\tau_1,\tau_c) = \mathbf{T}_{d\tau}\,\mathbf{d}'(\tau_1,\tau_c) + \mathbf{S}_{d\tau}\mathbf{u}'(\tau_1,\tau_c).$$

With substitution of Eq. (1),

$$\begin{aligned}\mathbf{u}(\tau_1,\tau_c) &= [(\mathbf{S}_{d\tau} + \mathbf{T}_{d\tau}\,\mathbf{S}_2^a)(\mathbf{I} + (\mathbf{S}_1^b\mathbf{S}_2^a) + (\mathbf{S}_1^b\mathbf{S}_2^a)^2 + \cdots)(\mathbf{T}_1^a + \mathbf{E}_1)]\mathbf{v}_{inc}\\ &= \mathbf{U}(\tau_1,\tau_c)\mathbf{v}_{inc},\\ \mathbf{d}(\tau_1,\tau_c) &= [(\mathbf{T}_{d\tau} + \mathbf{S}_{d\tau}\mathbf{S}_2^a)(\mathbf{I} + (\mathbf{S}_1^b\mathbf{S}_2^a) + (\mathbf{S}_1^b\mathbf{S}_2^a)^2 + \cdots)(\mathbf{T}_1^a + \mathbf{E}_1)]\mathbf{v}_{inc}\\ &= \mathbf{D}(\tau_1,\tau_c)\mathbf{v}_{inc},\end{aligned} \tag{2}$$

where the newly introduced matrices $\mathbf{U}, \mathbf{D}$ are of primary interest since in the present application of an incident solar illumination, $\mathbf{v}_{inc}$ just serves to sift out the appropriate column of those two matrices.

3.2. *The escape matrices for intensity at optical depth $\tau = \tau_1$, for a cloud with total optical thickness $\tau_c = \tau_1 + \tau_2$*

Now that the net upward and downward intensities at the $d\tau$ layer, $\mathbf{u}$ and $\mathbf{d}$, respectively, have been determined, we need to calculate the fraction of these intensities which escape out cloud top or base and contribute to the overall reflected and transmitted signal. This fraction accounts for the transport of intensities $\mathbf{u}$ and $\mathbf{d}$ to the cloud boundaries and can be represented in our present mathematical framework by *escape matrices*, designated as $\mathbf{Q}_u^r, \mathbf{Q}_u^t, \mathbf{Q}_d^r, \mathbf{Q}_d^t$ respectively. The superscripts r and t are used to represent an escape matrix for transport contributing to reflectance (i.e., transport out the top of the cloud) and transmittance (transport out the bottom), respectively; subscripts indicate transport of the upward or downward intensity vector. So the component of reflected intensity due to photons which have had a scattering in the infinitesimal layer is $\mathbf{Q}_u^r\mathbf{u} + \mathbf{Q}_d^r\mathbf{d} = (\mathbf{Q}_u^r\mathbf{U} + \mathbf{Q}_d^r\mathbf{D})\mathbf{v}_{inc}$; the transmitted component is $\mathbf{Q}_u^t\mathbf{u} + \mathbf{Q}_d^t\mathbf{d} = (\mathbf{Q}_u^t\mathbf{U} + \mathbf{Q}_d^t\mathbf{D})\mathbf{v}_{inc}$. These matrices depend on the surface reflectance beneath the cloud. For now, we assume a black surface. Accounting for multiple reflections between the two finite cloud layers, the superposition formulae for the escape matrices at the optical depth τ_1 are given by

$$\begin{aligned}\mathbf{Q}_u^r(\tau_1,\tau_c) &= (\mathbf{T}_1^b + \mathbf{E}_1)(\mathbf{I} + (\mathbf{S}_2^a\mathbf{S}_1^b) + (\mathbf{S}_2^a\mathbf{S}_1^b)^2 + \cdots),\\ \mathbf{Q}_d^r(\tau_1,\tau_c) &= (\mathbf{T}_1^b + \mathbf{E}_1)(\mathbf{I} + (\mathbf{S}_2^a\mathbf{S}_1^b) + (\mathbf{S}_2^a\mathbf{S}_1^b)^2 + \cdots)\mathbf{S}_2^a,\\ \mathbf{Q}_u^t(\tau_1,\tau_c) &= (\mathbf{T}_2^a + \mathbf{E}_2)(\mathbf{I} + (\mathbf{S}_1^b\mathbf{S}_2^a) + (\mathbf{S}_1^b\mathbf{S}_2^a)^2 + \cdots)\mathbf{S}_1^b,\\ \mathbf{Q}_d^t(\tau_1,\tau_c) &= (\mathbf{T}_2^a + \mathbf{E}_2)(\mathbf{I} + (\mathbf{S}_1^b\mathbf{S}_2^a) + (\mathbf{S}_1^b\mathbf{S}_2^a)^2 + \cdots).\end{aligned} \tag{3}$$

This reduces to the homogeneous cloud case derived by Twomey [9] and applied to the emergence of thermal radiation from within a cloud.

3.3. The number of scatterings in an infinitesimal layer at an optical depth of $\tau = \tau_1$, for a cloud with total optical thickness $\tau_c = \tau_1 + \tau_2$

The product of Eq. (3) premultiplying Eq. (2) represents the differential part of the total reflected and transmitted *intensities* consisting of photons having undergone a scattering in the infinitesimal layer. Specifically, these photons have scattered just once within the layer since the derivation assumes that higher-order scatterings become insignificant as the layer is made arbitrarily small. Since the *number of photons* traveling in some direction (solid angle) is proportional to intensity, normalizing the above differential intensity by the total intensity in the same exit direction is equivalent to the *fraction* of all such directed photons having one scattering in a layer $d\tau$, located at an optical depth τ, in a medium of total thickness τ_c. We can introduce a vertical distribution function $\zeta^r(\tau,\tau_c)$ such that $\zeta^r(\tau,\tau_c)\,d\tau$ gives this fraction for reflected photons, and a similar function $\zeta^t(\tau,\tau_c)\,d\tau$ describing the transmitted fraction. Including an explicit directional dependence in the matrix notation, the fraction of photons that have a scattering in the infinitesimal layer and go on to contribute to a bidirectional reflectance or transmittance signal, are given by

$$\zeta^r(\tau,\tau_c,\mu_i,\mu_j)\,d\tau = \frac{\{\mathbf{Q}_u^r(\tau,\tau_c)\mathbf{U} + \mathbf{Q}_d^r(\tau,\tau_c)\mathbf{D}\}_{i,j}}{S_{i,j}(\tau_c)} = \frac{\{\mathbf{Z}^r(\tau,\tau_c)\}_{i,j}}{S_{i,j}(\tau_c)}$$

$$\zeta^t(\tau,\tau_c,\mu_i,\mu_j)\,d\tau = \frac{\{\mathbf{Q}_u^t(\tau,\tau_c)\mathbf{U} + \mathbf{Q}_d^t(\tau,\tau_c)\mathbf{D}\}_{i,j}}{T_{i,j}(\tau_c) + E_{i,j}(\tau_c)} = \frac{\{\mathbf{Z}^t(\tau,\tau_c)\}_{i,j}}{T_{i,j}(\tau_c) + E_{i,j}(\tau_c)}, \tag{4a}$$

where the $\mathbf{Z}$ matrices are introduced for convenience, and μ_i and μ_j are the cosine of the zenith viewing and solar angle, respectively. We can also define similar fractions for photons contributing to albedo and flux transmittance by integrating both numerators and denominators over a hemisphere (summation over μ_i as described in Section 2), i.e.,

$$\zeta^r(\tau,\tau_c,\mu_j)\,d\tau = \frac{\sum_{i=1}^N \mu_i \{\mathbf{Z}^r(\tau,\tau_c)\}_{i,j}}{\sum_{i=1}^N \mu_i S_{i,j}(\tau_c)},$$

$$\zeta^t(\tau,\tau_c,\mu_j)\,d\tau = \frac{\sum_{i=1}^N \mu_i \{\mathbf{Z}^t(\tau,\tau_c)\}_{i,j}}{\sum_{i=1}^N \mu_i (T_{i,j}(\tau_c) + E_{i,j}(\tau_c))}. \tag{4b}$$

Eq. (4b) gives the fraction of the reflected and transmitted *flux* consisting of photons having undergone a scattering in the infinitesimal layer. Finally, on substitution of Eqs. (2) and (3), we can write

$$\begin{aligned}\mathbf{Z}^r(\tau,\tau_c) &= (\mathbf{T}_1^b + \mathbf{E}_1)(\mathbf{I} + (\mathbf{S}_2^a\mathbf{S}_1^b) + \cdots)[\mathbf{S}_{d\tau} + \mathbf{T}_{d\tau}\mathbf{S}_2^a + \mathbf{S}_2^a(\mathbf{T}_{d\tau} + \mathbf{S}_{d\tau}\mathbf{S}_2^a)] \\ &\quad \times (\mathbf{I} + (\mathbf{S}_1^b\mathbf{S}_2^a) + \cdots)(\mathbf{T}_1^a + \mathbf{E}_1), \\ \mathbf{Z}^t(\tau,\tau_c) &= (\mathbf{T}_2^a + \mathbf{E}_2)(\mathbf{I} + (\mathbf{S}_1^b\mathbf{S}_2^a) + \cdots)[\mathbf{T}_{d\tau} + \mathbf{S}_{d\tau}\mathbf{S}_2^a + \mathbf{S}_1^b(\mathbf{T}_{d\tau}\mathbf{S}_2^a + \mathbf{S}_{d\tau})] \\ &\quad \times (\mathbf{I} + (\mathbf{S}_1^b\mathbf{S}_2^a) + \cdots)(\mathbf{T}_1^a + \mathbf{E}_1),\end{aligned} \tag{5}$$

where the differential terms are given in Section 2. Though Eq. (5) may appear a bit intimidating, it can be easily integrated into existing adding/doubling codes which already contain similar calculations.

3.4. The average number of scatterings in a finite layer

By definition, Eqs. (4a) and (4b) give the total number of reflected (transmitted) photons, either passing through a hemisphere or into a particular direction, which have had a scattering in the layer $d\tau$, divided by the corresponding total number of reflected (transmitted) photons. So this quantity is also the *average number of scatterings* in the layer experienced by all such reflected or transmitted photons. This average must be much less than one since the layer is made infinitesimally thin and only single scattering events can occur.

The average number of reflected photons with scatterings in a finite layer between τ_a and τ_b is therefore given by the integration of Eq. (4) from τ_a to τ_b, which may now be greater than one since more than one scattering may occur in the finite layer for each photon. Likewise, the average number of scatterings for all reflected and transmitted photons, N_s^r and N_s^t, respectively, in a medium with total optical thickness τ_c, can be found from

$$N_s^r = \int_0^{\tau_c} \zeta^r(\tau,\tau_c)\,d\tau,$$

$$N_s^t = \int_0^{\tau_c} \zeta^t(\tau,\tau_c)\,d\tau, \tag{6}$$

where the directional dependence of either Eq. (4a) (average number of scatterings for photons into viewing direction μ_i) or Eq. (4b) (average number of scatterings for photons into a hemisphere) is understood; in both cases the solar flux is incident from the μ_j direction. The integrals should be recognized as averages for a large number of reflected or transmitted photons.

Photon counts are equivalent to flux, not intensity. Accordingly, Eqs. (4a) and (4b) are consistent with the average number of photon scatterings into a hemisphere being the flux-weighted average of the average number of scatterings into viewing directions μ, i.e.,

$$N_{s,\text{Hemisphere}} = \frac{\int_0^1 \mu I(\mu) N_s(\mu)\,d\mu}{\int_0^1 \mu I(\mu)\,d\mu} \equiv \frac{\sum_{i=1}^N \mu_i I(\mu_i) N_s(\mu_i)}{\sum_{i=1}^N \mu_i I(\mu_i)} \tag{7}$$

where I is the intensity, azimuthal variability is ignored, and the summation over all μ_i bins gives the vector–matrix implementation.

A non-zero surface reflectance is accounted for via Eq. (5) by replacing $\mathbf{S}_2^a$ with the reflectance matrix found from superposition of layer 2 over a surface described by reflectance matrix $\mathbf{S}_{sfc}$. This leads to the modification

$$\mathbf{S}_2^a \to \mathbf{S}_2^a + (\mathbf{T}_2^b + \mathbf{E}_2)\mathbf{S}_{sfc}(\mathbf{I} + \mathbf{S}_2^b\mathbf{S}_{sfc} + (\mathbf{S}_2^b\mathbf{S}_{sfc})^2 + \cdots)(\mathbf{T}_2^a + \mathbf{E}_2).$$

Likewise, the net layer 2 transmittance $(\mathbf{T}_2^a + \mathbf{E}_2)$ is now enhanced by multiple reflections off the surface, becoming

$$(\mathbf{T}_2^a + \mathbf{E}_2) \to (\mathbf{I} + \mathbf{S}_2^b\mathbf{S}_{sfc} + (\mathbf{S}_2^b\mathbf{S}_{sfc})^2 + \cdots)(\mathbf{T}_2^a + \mathbf{E}_2).$$

The result is that both reflected and transmitted photons have more scatterings, especially in lower layers of the cloud (see Fig. 4 in the following section).

There is reciprocity upon exchange of solar and viewing directions for the bidirectional form of these equations. Though we have purposely ignored any mention of the sign of μ, it is useful to do

so now, especially in discussion of the transmittance weighting. Let propagation in a downward direction correspond to $-1 \leq \mu < 0$ and propagation in an upward direction to $0 < \mu \leq 1$ (following Chandrasekhar [11]). The reflectance scattering distribution can then be written more explicitly as $\zeta^r(\tau, \tau_c, +|\mu|, -|\mu_0|)$ indicating downward propagating incident radiation scattered back into the upward hemisphere. Reciprocity for the reflectance weighting then becomes $\zeta^r(\tau, \tau_c, +|\mu|, -|\mu_0|) = \zeta^r(\tau, \tau_c, +|\mu_0|, -|\mu|)$. Transmitted radiation emerges into the same hemispheric direction as the incident, and so the weighting function is written as $\zeta^t(\tau, \tau_c, -|\mu|, -|\mu_0|)$ for radiation incident at cloud top. The reciprocity relation for the transmittance weighting is then given by the $\zeta^t(\tau, \tau_c, -|\mu|, -|\mu_0|) = \zeta^t(\tau, \tau_c, +|\mu_0|, +|\mu|)$, where the latter function describes upward propagating radiation incident at cloud base. Note that an exchange of directions for transmittance involves both a sign change and angle substitution. If the cloud is homogeneous, then transmittance functions and weightings for radiation incident from both above and below the cloud, at the same set of angles, are equivalent with respect to the incident level, i.e., $\zeta^t(\tau, \tau_c, -|\mu|, -|\mu_0|) = \zeta^t(\tau_c - \tau, \tau_c, +|\mu|, +|\mu_0|)$ and therefore reciprocity extends to $\zeta^t(\tau, \tau_c, -|\mu|, -|\mu_0|) = \zeta^t(\tau_c, -\tau, \tau_c, -|\mu_0|, -|\mu|)$. In other words, the transmittance scattering distribution for homogeneous clouds is simply inverted with respect to optical depth upon exchange of angles in the same hemisphere. The last statement turns out to be approximately true even for the inhomogeneous clouds discussed in the next section. Similarly, normalizations of the scattering number distributions, N_s^r and N_s^t, also obey reciprocity.

Though the preceding derivation was developed for use in cloud remote sensing problems, it is applicable to any plane-parallel, vertically inhomogeneous, multiple scattering medium illuminated by a plane-parallel flux. General incident illuminations can be handled by properly specifying the incident intensity vector $\mathbf{v}_{inc}$ and making corresponding summations over the index j. While only the azimuthally averaged component of the radiation field is explicitly considered, Fourier components can be added to the adding/doubling formulation in the usual manner.

4. Results and Monte Carlo comparisons

The vertical distribution of the average number of scatterings is shown in Fig. 2 for reflected and transmitted photons in four solar spectral bands commonly used in cloud remote sensing (0.66, 1.6, 2.2, and 3.7 μm). Calculations are for the bidirectional case (Eq. (4a)) and a homogeneous liquid water cloud of optical thickness 8. Cloud droplet sizes are described by a gamma distribution [10] with a 10 μm effective radius and an effective variance of 0.10. Other details of the solar/viewing geometry are given in the caption. Since optical path is wavelength dependent through the extinction efficiency, Q_e, both the optical thickness and ordinate are given as the path amount after scaling to a common extinction efficiency of 2.0 (i.e., $\tau \to 2\tau/Q_e$). In this way, scattering number distributions can be directly compared among the four spectral bands. The liquid water droplet single scattering parameters in these bands, averaged over typical imaging instrument spectral response functions used in cloud remote sensing [12], are given in Table 1. Droplet absorption is seen to increase with band wavelength, from zero in the visible to 10% in the 3.7 μm band.

The vertical distribution for reflected photons in Fig. 2 peaks just below cloud top and then decreases towards cloud base. This is in contrast to the transmittance distribution which is

Table 1
Scattering parameters averaged over typical cloud remote sensing instrument spectral response functions, for a cloud droplet size spectra given by a gamma distribution with an effective radius of 10 μm and a 0.10 effective variance

Spectral band (μm)	Single scattering albedo, $\bar{\omega}_0$	Asymmetry parameter, g	Extinction efficiency, Q_e
0.66	1.000	0.861	2.10
1.6	0.994	0.843	2.19
2.2	0.979	0.834	2.25
3.7	0.900	0.794	2.33

relatively symmetric with optical depth, showing a broad maximum throughout the middle layers of the cloud. Scattering numbers are seen to decrease with droplet absorption as expected. The integral of the distributions (Eq. (6)) gives the average number of scatterings for all photons directed into the viewing direction, and is shown in the legend. Both superposition and Monte Carlo calculations are shown in Fig. 3 for the 2.2 μm band and the same cloud and geometry of Fig. 2. In order to compare directly with the 20-stream implementation of the superposition matrix formulation (see Section 2), Monte Carlo statistics are collected for solar and viewing angular bin sizes of $\Delta\mu = \pm 0.05$. A relatively small discrepancy is seen for reflectance numbers near cloud top and a small offset for transmittance numbers. However, this difference disappears when the scattering number distribution for reflected flux (albedo) and transmitted flux is compared, suggesting some small difference in the implementation of the phase function in the two techniques.

The effect of a Lambertian surface reflectance of 0.30 on the flux vertical scattering distribution is shown in Fig. 4 for the visible band; for comparison, the distribution for a black surface is also shown. With the reflecting surface, scattering numbers increase in lower layers as photons reflected from the surface are returned towards cloud base. Though the total scattering number in the uppermost layers can never decrease by addition of a reflecting surface, the average number can. This explains the slight decrease near cloud top in the reflectance distribution plot. Evidently, the great majority of additional reflected photons resulting from surface scattering are those fortunate enough to get transmitted through the uppermost layers without a scattering. Since the total number of reflected photons increase with the addition of the reflecting surface, the average number in layers without additional scatterings decreases. Both cases are compared with Monte Carlo calculations and the agreement is seen to be excellent.

A vertical structure in droplet absorption (i.e., effective radius) can also influence the scattering distribution. This can be explored with the superposition formulae which can easily incorporate plane-parallel, vertically inhomogeneous layers. Fig. 5 shows the effect of several analytic vertical profiles of effective radius on the reflectance scattering distribution in the 2.2 μm band. The *linear* profile means linear with optical depth, for cloud base and cloud top effective radii of 5 and 12 μm, respectively. Using these same boundary conditions, the *adiabatic* distribution refers to the droplet size profile resulting from a cloud parcel rising along a moist adiabat. This gives liquid water concentration increasing linearly with geometric height, and for a constant number of cloud

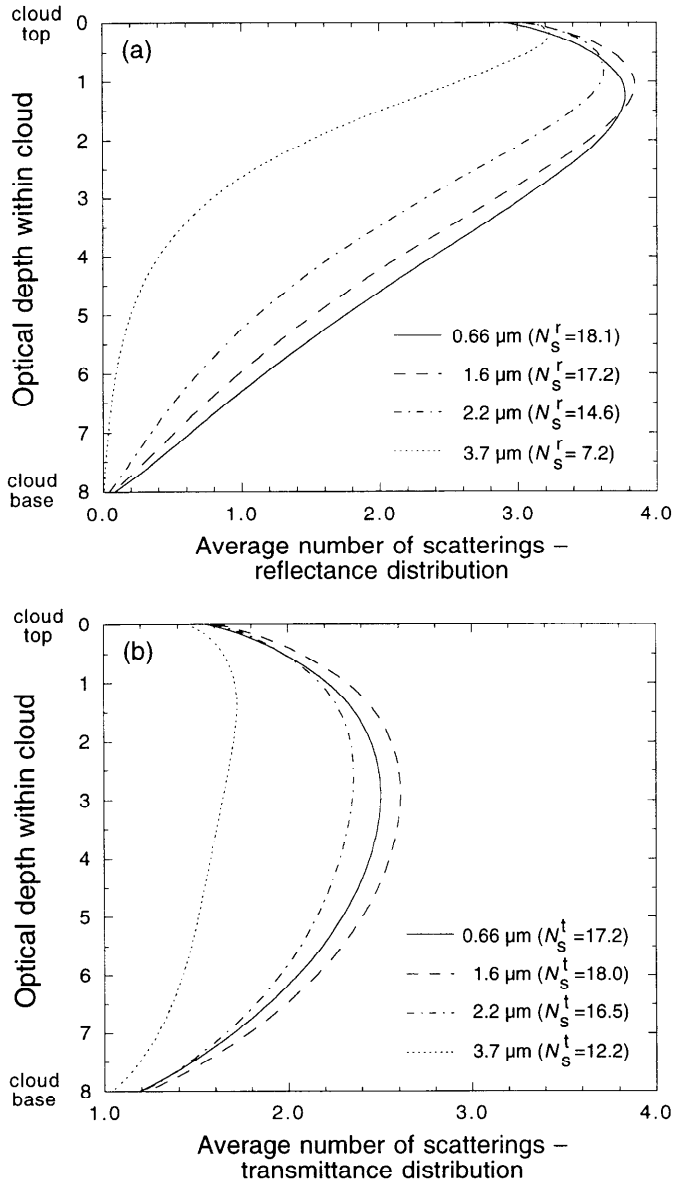

Fig. 2. Vertical distribution of the average number of scatterings per differential layer for (a) reflected, and (b) transmitted photons in four spectral bands from 0.66 to 3.7 μm. Calculated for a homogeneous cloud with optical thickness 8 and a droplet effective radius of 10 μm, cosine of solar and viewing angles of $\mu_0 = 0.65$ and $\mu = 0.85$, respectively, and an azimuthal average. N_s^r and N_s^t refer to the average number of scatterings for all reflected and transmitted photons, respectively, found by integrating the distributions.

droplets, effective radius decreasing towards cloud base as $(a_0 - a_1\tau)^{1/5}$ where the a's are constants determined by the boundary conditions. Reflected photons penetrate deeper into the cloud for the linear size profile as smaller effective radii, and therefore less absorption, are found at higher levels.

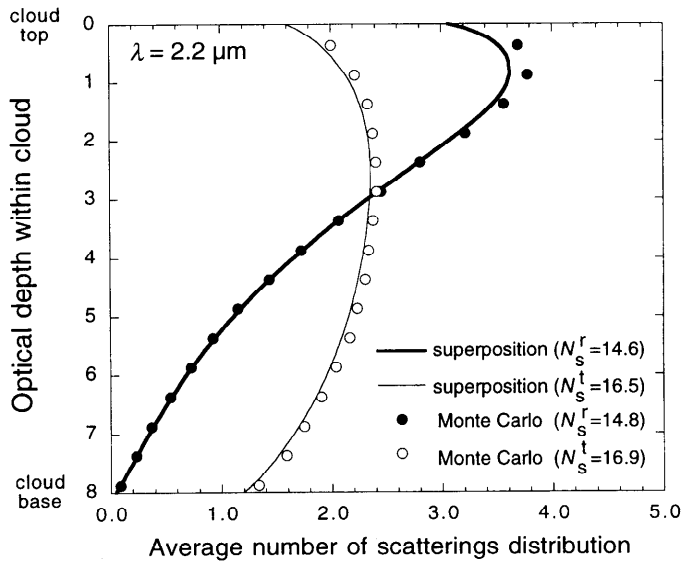

Fig. 3. Vertical distribution of the average number of scatterings per differential layer for reflected and transmitted photons in a 2.2 μm spectral band. Results using superposition formulae (lines) are compared with Monte Carlo calculations (symbols) for the cloud model and geometry described in Fig. 2. Monte Carlo results are averaged over angular bin sizes of $\Delta\mu = \pm 0.05$. N_s^r and N_s^t refer to the average number of scatterings for all reflected and transmitted photons, respectively.

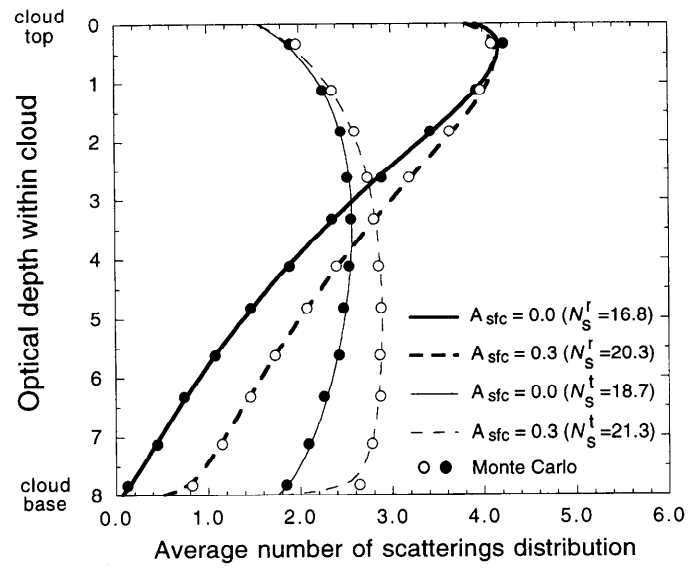

Fig. 4. Dependence of the scattering number distribution on Lambertian surface albedo (A_{sfc}) in a visible band (0.66 μm) showing both superposition formulae and Monte Carlo results. Calculations are made for $\mu_0 = 0.65$, flux reflectance (albedo) and transmittance, and the cloud model described in Fig. 2. N_s^r and N_s^t refer to the average number of scatterings for all reflected and transmitted photons, respectively.

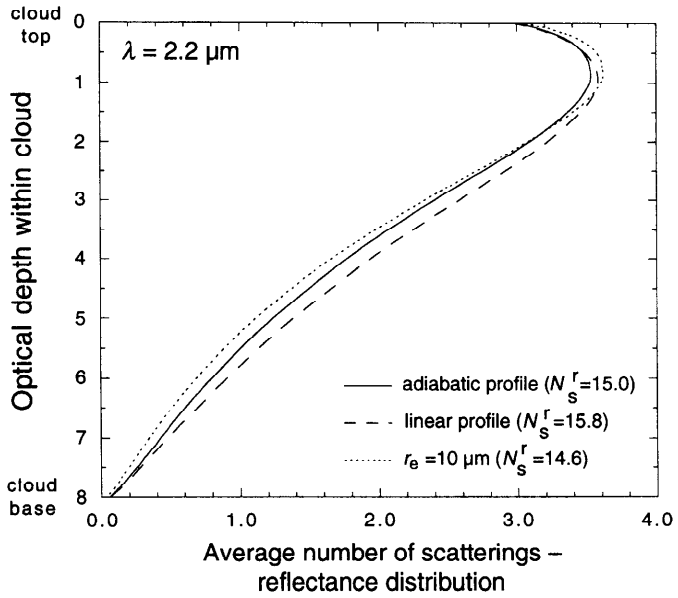

Fig. 5. Vertical distribution of the average number of scatterings per differential layer for reflected photons in a 2.2 μm spectral band as a function of three effective radius profiles discussed in the text. Calculated for the cloud model and geometry described in Fig. 2.

The distribution for a homogeneous cloud with effective radius 10 μm is also shown. Though the differences between the curves appear slight, they may give rise to noticeable discrepancies in droplet size remote sensing retrievals [13].

A final check of the superposition formulae is to compare the average number of scatterings for the entire cloud, N_s^r and N_s^t, with Monte Carlo calculations across a large range of optical thicknesses and droplet absorption. These comparisons are shown in Fig. 6. The agreement is excellent, and comparable with results from other studies [4,5,7].

5. Applications

An efficient method for determining photon scatterings in individual layers of a vertically structured cloud is interesting in its own right. In addition, such calculations can aid in understanding the effect of heterogeneous clouds fields on remote sensing problems by giving the relevant scales over which homogeneous, plane-parallel assumptions need be valid.

A normalized vertical scattering distribution gives information regarding the relative influence of individual layers on the path history of photons. This distribution may then be used to qualitatively understand, if not estimate, the effect of vertical cloud inhomogeneity on the remote sensing of cloud effective radii from solar reflectance measurements [13]. Such retrievals use the same visible and near-infrared bands discussed in the previous section. Since Eq. (6) is the normalization for the function ζ, a normalized weighting function proportional to the number of scatterings in each

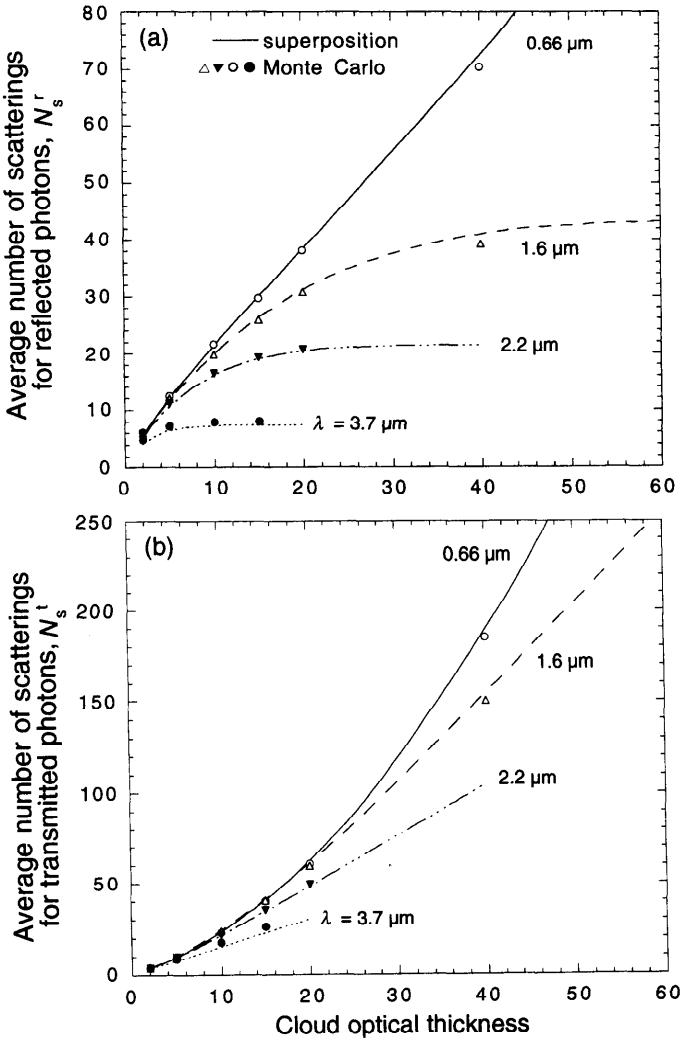

Fig. 6. Average number of scatterings for all (a) reflected, and (b) transmitted photons as a function of cloud optical thickness in four spectral bands. Monte Carlo calculations (symbols) are compared with superposition calculations (lines) for a homogeneous cloud with an effective radius of 10 μm, and the geometry of Fig. 2. Monte Carlo results are averaged over angular bin sizes of $\Delta\mu = \pm 0.05$.

vertical layer is given as:

$$w^r(\tau,\tau_c) = \frac{\zeta^r(\tau,\tau_c)}{N_s^r},$$

$$w^t(\tau,\tau_c) = \frac{\zeta^t(\tau,\tau_c)}{N_s^t}. \tag{8}$$

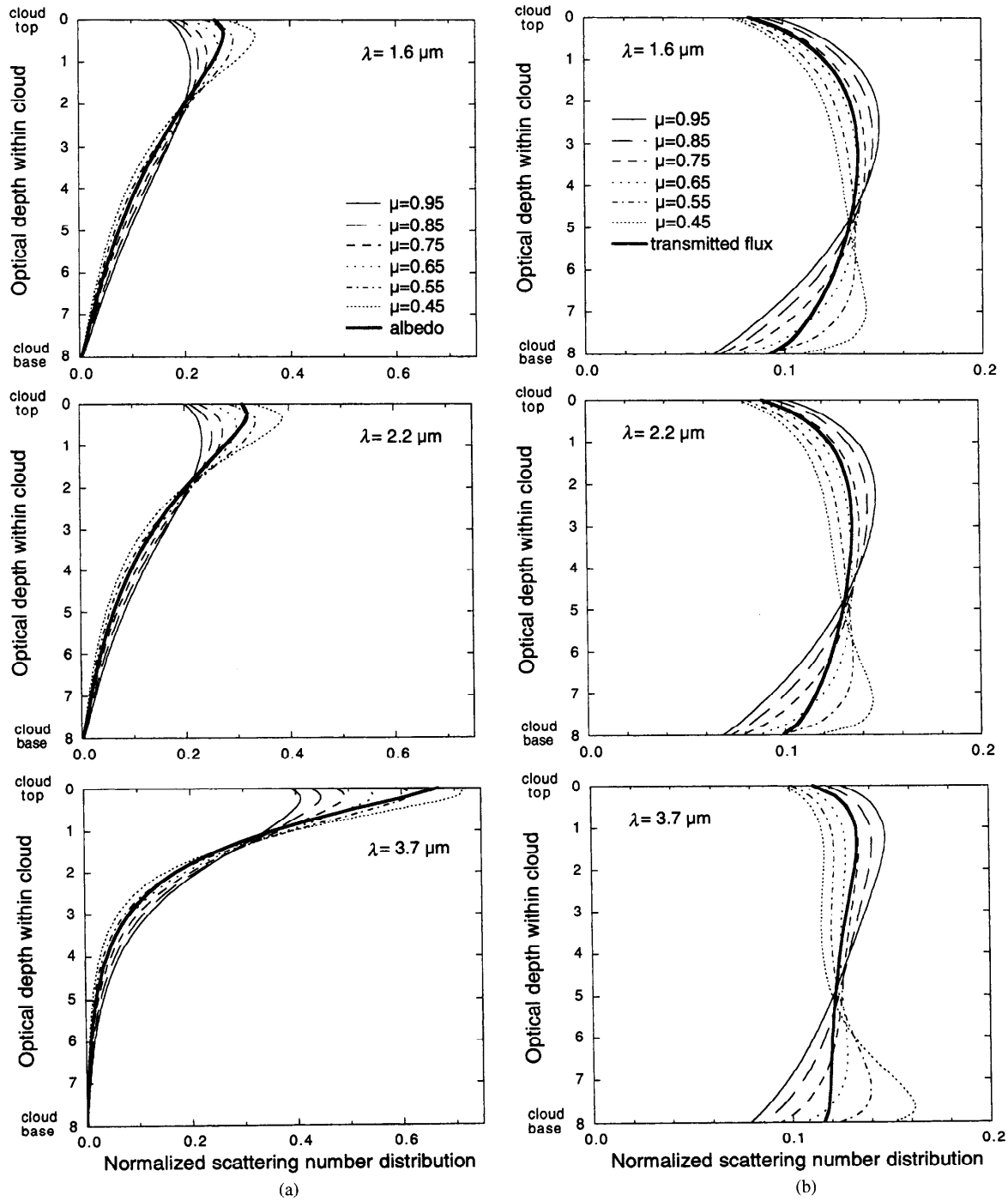

Fig. 7. (a) Dependence of the normalized scattering number distribution for bidirectional reflectance on the cosine of the viewing angle, μ, for the three near-infrared bands of Table 1, $\mu_0 = 0.65$, and a homogeneous cloud with effective radius 10 μm. The distribution for reflected flux, or albedo, is also shown. (b) Same as Fig. 7(a), but for bidirectional and flux transmittance.

The directional dependence is understood, coming into play via Eqs. (4a) and (4b). Examples of these functions are shown in Fig. 7 for the three cloud droplet absorbing bands as a function of bidirectional viewing angle as well as the hemispheric view. Though calculations are for a homogeneous cloud with 10 μm effective radii, the effective radius profiles of Fig. 5 would give similar looking normalized distributions. As expected, there are relatively more scatterings near cloud top as both reflectance zenith viewing angle and droplet absorption increase (Fig. 7a). A sensor viewing a vertically structured cloud with these bands from the more oblique angles would therefore infer a droplet size representative of higher levels in the cloud compared with nadir view. Similarly for transmittance where viewing angle now refers to an observer below cloud (Fig. 7b). The hemispheric flux results are also shown.

For horizontal transport, the root-mean-square displacement of reflected and transmitted photons in a plane-parallel, vertically inhomogeneous medium can be estimated from diffusion theory if the average number of photon scatterings is known [13]. Such diffusive transport is therefore derivable from the same efficient superposition formula already presented. This horizontal displacement can then be used to assess the scales over which horizontal inhomogeneities are important in remote sensing problems. A detailed discussion of horizontal transport in visible and near-infrared remote sensing bands, using results from the current work, is presented in an accompanying paper [14].

6. Conclusions

The average number of scatterings in an arbitrary layer of a plane-parallel, inhomogeneous cloud has been derived from superposition principles. The formulae have been couched in adding and doubling radiative transfer notation, and can therefore be implemented in a straightforward way from existing adding/doubling code. Calculations have been made for bidirectional reflectance and transmittance from a liquid water droplet cloud at various combinations of solar and viewing angles, as well as for reflected and transmitted flux. Results were shown for typical reflectance-based cloud remote sensing spectral bands located in atmospheric windows from the visible (conservative scattering) through the near-infrared (significant droplet absorption). Selected results have been compared with time-intensive Monte Carlo calculations, and the agreement was found to be excellent. Though the current effort was limited to the azimuthally averaged component of the radiation field, a Fourier expansion can be included in the adding/doubling formulation.

This simple and fast method for determining photon scatterings in individual layers of a vertically structured cloud as a function of solar and viewing geometry, has application to remote sensing problems of inhomogeneous cloud fields. One such example is the retrieval of cloud droplet effective radius in vertically inhomogeneous clouds. Average scattering statistics are also useful in estimating horizontal transport in plane-parallel clouds. Though the emphasis has been on terrestrial cloud remote sensing problems, the superposition formulae are applicable to any plane-parallel, vertically inhomogeneous, multiple scattering medium with arbitrary illumination.

Acknowledgements

This work was supported in part by grant NAG5-6996 from the National Aeronautics and Space Administration, EOS validation program office. The author wishes to thank Dr. A. Davis for helpful comments.

References

[1] van de Hulst HC. Multiple light scattering. New York: Academic Press, 1980.
[2] Pfeilsticker K, Erle F, Funk O, Veitel H, Platt U. First geometrical pathlengths probability density function derivation of the skylight from spectroscopically highly resolving oxygen A-band observations: 1. Measurement technique, atmospheric observations and model calculations. J Geophys Res 1998;103:11483–504.
[3] Weinman JA. Effects of multiple scattering on light pulses reflected by turbid atmospheres. J Atmos Sci 1976;33:1763–71.
[4] Plass GN, Kattawar GW. Reflection of light pulses from clouds. Appl Opt 1971;10:2304–10.
[5] Plass GN, Kattawar GW. Monte Carlo calculations of light scattering from clouds. Appl Opt 1967;7:415–9.
[6] Viik T. Average photon path-length of radiation emerging from finite atmospheres: I. Henyey-Greenstein phase function. Astrophys Space Sci 1995;232:37–48.
[7] Twomey S, Jacobowitz H, Howell HG. Light scattering by cloud layers. J Atmos Sci 1967;24:109–18.
[8] Twomey S, Jacobowitz H, Howell HG. Matrix methods for multiple-scattering problems. J Atmos Sci 1966;23:101–8.
[9] Twomey S. Doubling and superposition methods in the presence of thermal emission. JQSRT 1979;22:355–63.
[10] Hansen JE, Travis LD. Space. Sci Rev 1974;31:527.
[11] Chandrasekhar S. Radiative transfer. New York: Dover Press, 1960.
[12] Platnick S, Durkee PA, Nielsen K, Taylor JP, Tsay SC, King MD, Ferek RJ, Hobbs PV, Rottman JW. The role of background cloud microphysics in the radiative formation of ship tracks. J Atmos Sci 2000, in press.
[13] Platnick S. The scales of photon transport in cloud remote sensing problems. In: Smith WL, Stamnes K, editors. IRS '96: current problems in atmospheric radiation. Hampton, Virginia: A. Deepak, 1997, p. 206–9.
[14] Platnick S. Approximations for horizontal photon transport in cloud remote sensing problems. JQSRT 2001;68:75–99.